

## VIP Very Important Paper

## Photo-Activity of Silacyclopropenes and their Application in Metal-Free Curing of Silicones

Matthias Nobis,<sup>[a, b]</sup> Jonas Futter,<sup>[b]</sup> Maximilian Moxter,<sup>[c]</sup> Shigeyoshi Inoue,<sup>[a]</sup> and Bernhard Rieger<sup>\*[a, b]</sup>

Silicone elastomers are usually produced via addition or condensation curing by means of platinum- or tin-based catalysis. The employed catalysts remain in the final rubber and cannot be recovered, thus creating various economic and environmental challenges. Herein, a light-mediated curing method using multifunctional silacyclopropenes as crosslinker structures was introduced to create an effective alternative to the conventional industrial crosslinking. To evaluate the potential of the photoreaction a model study with small monofunctional silirenes was conducted. These investigations confirmed the required coupling reactivity upon irradiation and

revealed an undesired rearrangement formation. Further optimization showed the reaction selectivity to be strongly influenced by the substitution of the three-membered ring system and the reaction temperature. The synthesis of multifunctional silirenes was described based on the most suitable model compound to create active crosslinker scaffolds for their application in silicone curing. This photo-controlled process produces catalyst and additive free elastomers from liquid silicones, including hydride-, hydroxy-, or vinyl terminated polydimethylsiloxanes.

## Introduction

One of the most relevant inorganic polymers is the class of polysiloxanes commonly known as silicones. They can be found in a vast range of applications due to their outstanding physical and mechanical properties, as well as their thermal robustness and chemical stability.<sup>[1]</sup> This renders this material dominant across a variety of sectors from the construction, automotive, textile, and cosmetic to pharmaceutical and biomedical industries.<sup>[2]</sup> While silicones are used as fluids, gels, or resins, the segment of cured elastomers led the global silicone market with a share of more than 41% in 2020.<sup>[3]</sup> Conventional crosslinking strategies are centered on the addition (hydrosilylation) or condensation curing of polydimethylsiloxane (PDMS). Silicone rubber created via condensation is inexpensive and easy to handle; however, volatile elimination products and long curing durations restrict its application. Although addition

curing benefits from fast crosslinking reactions and low network shrinkage, it is limited to a more expensive two-component mixture of hydride- and vinyl-functionalized PDMS. Both techniques share the need for a metal catalyst such as platinum (addition) or tin (condensation) to cure PDMS at room temperature.<sup>[4]</sup> Furthermore, the implemented metal catalysts and respective degradation products will remain in the final silicone network, thus creating economic challenges and raising environmental questions. Even though catalyst amounts could be reduced to ppm concentrations by improving catalyst design,<sup>[5]</sup> the thriving demand for silicone elastomers results in the waste of 4–6 tons of pure platinum each year.<sup>[6]</sup> All this emphasizes the necessity for novel metal-free crosslinking methods. Alternative curing via autoxidation,<sup>[7,8]</sup> silacyclopropanes,<sup>[9]</sup> thiol-enes,<sup>[10]</sup> polysilazanes,<sup>[11]</sup> or cyclic disulfides<sup>[12]</sup> has been introduced over the past years. While autoxidative curing can use readily available hydride-terminated silicones, it is restricted to temperatures above 220 °C.<sup>[8]</sup> Another heat-controlled method is the curing of hydroxy-terminated PDMS by using silacyclopropanes in a ring-opening reaction. Respective UV-based curing can be realized by using thiol-ene-functionalized polysiloxanes as crosslinkers to create soft PDMS-networks with vinyl-terminated silicones.<sup>[10]</sup> Comparable efforts to cure with UV-light were made by employing cyclic disulfides as terminal functionalities on the PDMS chains. Further ring-opening polymerization afforded the respective bottlebrush elastomers.<sup>[12]</sup> All of these methods are limited by either high temperatures or the necessity of a specific PDMS functionality. To tackle these issues, we wanted to create a catalyst-free method, which can be applied at room temperature for a broad range of commonly used PDMS functionalities.

For this, we introduce a curing strategy by utilizing multifunctional silacyclopropenes (silirenes) as crosslinker scaffolds. Collin and Gaspar reported the first synthesis of a silacyclopro-

[a] M. Nobis, Prof. Dr. S. Inoue, Prof. Dr. B. Rieger  
WACKER-Institute of Silicon Chemistry  
Technical University of Munich  
85747 Garching bei München (Germany)  
E-mail: rieger@tum.de

[b] M. Nobis, J. Futter, Prof. Dr. B. Rieger  
WACKER-Chair of Macromolecular Chemistry  
Technical University of Munich  
85747 Garching bei München (Germany)

[c] Dr. M. Moxter  
Consortium für elektrochemische Industrie  
WACKER Chemie AG  
Zielstattstraße 20, 81379 München (Germany)

Supporting information for this article is available on the WWW under <https://doi.org/10.1002/cssc.202201957>

© 2022 The Authors. ChemSusChem published by Wiley-VCH GmbH. This is an open access article under the terms of the Creative Commons Attribution Non-Commercial License, which permits use, distribution and reproduction in any medium, provided the original work is properly cited and is not used for commercial purposes.

ene in 1976.<sup>[13]</sup> Since then the moiety of silirenes have gained considerable attention and various synthesis strategies have been reported. Most of them involve a [2 + 1] cycloaddition of an alkyne to the respective silylene.<sup>[14]</sup> These three-membered ring systems, known to undergo various reactions in response to heat<sup>[15,16]</sup> or UV irradiation,<sup>[15,17]</sup> serve as stable precursors for transient silylenes. The high reactivity of these silylenes ensures a fast curing reaction with the respective silicone functionalities to compete with the conventional crosslinking methods. The general feasibility of a silylene-based curing of linear PDMS was reported by our group in 2020.<sup>[9]</sup> However, the presented curing strategy can only be performed at high temperatures above 140 °C and limitations of the applicable silicone functionalities reduce its effectiveness and scope. By setting up a silirene-based crosslinking concept we are able to present a UV-light controlled curing for hydride-, hydroxy-, and vinyl-functionalized linear PDMS. In this work our aim is to combine the benefits of light-mediated, room-temperature curing with the expansion of employable silicone functionalities, yielding metal-, catalyst-, and additive-free silicone elastomers.

### Curing concept, design, and conditions

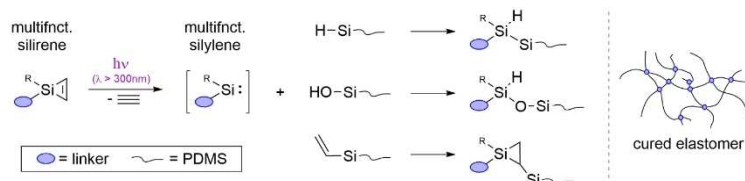
For creating a catalyst-free curing concept for silicones, we were drawn to the motif of silacyclopropenes. The three-membered ring of the silirene can be opened under UV-light to generate transient silylenes. These highly reactive low-valent silicon species can easily react with commonly used silicone functionalities like Si–H, Si–OH, or Si–vinyl.<sup>[15,18]</sup> We surmised that this reactivity could be used to crosslink the silicone chains and create the desired elastomers (Scheme 1). Additionally, the class of silirenes shows a high stability, compared, for example, to their saturated analogues, the silacyclopropanes.<sup>[19,20]</sup> This property is key for creating stable curing mixtures and a defined curing initiation. Furthermore, silirenes display characteristic absorption bands in the near ultraviolet regions, due to their “pseudo- $\pi$ ” aromatic ring-system.<sup>[19]</sup> This property is crucial, because although polysiloxanes exhibit an excellent transmittance in the visible and near-ultraviolet light spectrum, the absorbance of the polymer at wavelengths shorter than 280 nm increases significantly,<sup>[21]</sup> thus rendering all photo-based curing efforts below this limit improbable. Another benefit arises from the chemical composition of the silirene linker structures itself, which consist only of atoms already present in polysiloxanes.

Hence, we can avoid introducing additional heteroatoms and possibly deteriorating the final elastomer properties.

## Results and Discussion

### Model compounds

We began our search for an effective crosslinker by investigating suitable silirenes. Initial syntheses of small monofunctional silirenes as model compounds were performed to study potential candidates for the intended photoreactions. In order to synthesize a broad variety of silirenes **E1–E20** (Table 1), we employed the silylene-transfer reaction, by converting literature-known silacyclopropane **S1** in the presence of acetylenes **A1–A20**.<sup>[22]</sup> Commercially unavailable acetylenes were synthesized by literature-known procedures either via cross-coupling of bis(trimethylsilyl)acetylene,<sup>[23]</sup> reduction of tetrachloroethylene with lithium,<sup>[24]</sup> or treatment of trichloroethylene or phenylacetylene with *n*-butyllithium in combination with the respective halogen substrate.<sup>[25]</sup> The subsequent reaction to afford the respective silacyclopropene **E1–E20** could be realized either thermally ( $T > 120$  °C), or catalytically (AgOTf, 1.0 mol%). Best results were observed using a small excess (1.1 equiv.) of acetylene **A** compared to silirane **S1**. While higher yields were observed for the catalytically controlled reaction in most cases, phosphine-substituted silacyclopropene **E19** and **E20** could only be synthesized thermally. Further, no product formation could be noticed for silirenes **E6**, **E11**, and **E12** through the presented procedures. We surmise that with increasing steric demand of the acetylene the formation of the silacyclopropene becomes improbable and no reaction occurs, since this affects only acetylenes with larger substituents. We then conducted UV/Vis-measurement with the new silirenes **E1–E20** to assess their potential for a light induced reaction. We can conclude that the solely alkyl/aryl-substituted silacyclopropenes (**E1–E5**) show the lowest absorption maxima around 270 nm, whereas silyl-substituted silirenes (**E7–E10**) convene the highest observed absorption maxima from 324 up to 348 nm. Asymmetric Si/C-substituted silirenes (**E13–E17**) can be found between these two silirene classes, with absorption maxima located around 320 nm. This tendency can also be correlated to the respective chemical shifts in the <sup>29</sup>Si nuclear magnetic resonance (NMR) spectra. We observed that an upfield shift of the signal of the central silicon atom corresponds to an absorption maximum at higher wavelengths. We hypothesize that the



**Scheme 1.** Light-mediated curing strategy: multifunctional silirene scaffolds form PDMS elastomers with hydride-, hydroxy-, and vinyl-functionalized silicones via photo-induced generation of transient silylene-linkers.

**Table 1.** Overview of (a) the synthesis of model silirenes **E1–E20** via silylene transfer reaction with silirane **S1** and (b) the relative ratio of insertion (In) to rearrangement (Re) product in the photoreaction with triethylsilane.

| a  |                               |   |                            |   |                      |
|--|-------------------------------|---|----------------------------|---|----------------------|
| Silirane   |                               | A1-20   |                            | Silirene  |                      |
|                     |                               |  |                            |  |                      |
| <b>S1</b>  |                               | $\xrightarrow[\text{(toluene)}]{\Delta T / [\text{AgOTf}]}$                       |                            | <b>E1-20</b>  |                      |
| b  |                               |   |                            |   |                      |
| <b>E1-20</b>   |                               | Insertion   |                            | Rearrangement   |                      |
|                     |                               |  |                            |  |                      |
| $\xrightarrow[\text{(n-hexane)}]{\text{Et}_3\text{SiH (2 eq.)}, \text{h}\nu (\lambda_{\text{max}})}$ |                               | <b>In</b>   |                            | <b>Re1-20</b>   |                      |
| E  | R                             | R'  | Yield <sup>[a]</sup> E [%] | Abs. $\lambda$ [nm]   | In/Re <sup>[b]</sup> |
| 1  | Me                            | Me  | 78                         | 246   | 100:0                |
| 2  | Et                            | Et  | 72                         | 225   | 100:0                |
| 3  | Ph                            | Me  | 82                         | 260   | 100:0                |
| 4  | Ph                            | Ph  | 84                         | 290   | — <sup>[c]</sup>     |
| 5  | <i>m</i> -xylyl               | <i>m</i> -xylyl   | 45                         | 296   | — <sup>[c]</sup>     |
| 6  | <i>o</i> -xylyl               | <i>o</i> -xylyl   | — <sup>[d]</sup>           | —   | — <sup>[c]</sup>     |
| 7  | SiMe <sub>3</sub>             | SiMe <sub>3</sub>   | 75                         | 348   | 35:65                |
| 8  | SiMe <sub>2</sub> Et          | SiMe <sub>2</sub> Et  | 58                         | 324   | 34:66                |
| 9  | SiMe <sub>2</sub> tBu         | SiMe <sub>2</sub> tBu   | 60                         | 327   | 37:63                |
| 10   | SiEt <sub>3</sub>             | SiEt <sub>3</sub>   | 53                         | 328   | 33:67                |
| 11   | SiPh <sub>3</sub>             | SiPh <sub>3</sub>   | — <sup>[d]</sup>           | —   | —                    |
| 12   | Si( <i>i</i> Pr) <sub>3</sub> | Si( <i>i</i> Pr) <sub>3</sub>   | — <sup>[d]</sup>           | —   | —                    |
| 13   | SiMe <sub>3</sub>             | Me  | 65                         | 278   | 63:37                |
| 14   | SiMe <sub>3</sub>             | Ph  | 79                         | 325   | 65:35                |
| 15   | SiEt <sub>3</sub>             | Ph  | 70                         | 323   | 66:34                |
| 16   | SiMePh <sub>2</sub>           | Ph  | 55                         | 327   | 61:39                |
| 17   | Si( <i>i</i> Pr) <sub>3</sub> | Ph  | 58                         | 325   | 65:35                |
| 18   | GeMe <sub>3</sub>             | GeMe <sub>3</sub>   | 51                         | 333   | 0:100                |
| 19   | P(Ph) <sub>2</sub>            | P(Ph) <sub>2</sub>  | 57                         | 315   | — <sup>[c]</sup>     |
| 20   | P(Ph) <sub>2</sub>            | Ph  | 61                         | 325   | — <sup>[c]</sup>     |

[a] All yields given for isolated pure compounds. [b] Relative yields were calculated via <sup>1</sup>H and <sup>29</sup>Si NMR spectroscopy by comparing the respective integrals. [c] No photoreaction at any given wavelength (254–420 nm) could be observed. [d] No product formation was observed. Starting material could not be recovered.

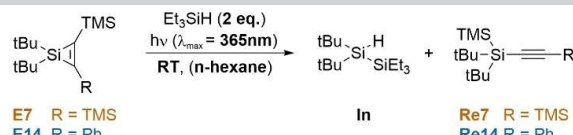
observed shielding effect is caused by an increase of electron density at the ring-system, which could shift the excitation of the silirene towards higher wavelengths.

### Si–H photoreactivity

To establish the desired reactivity, we tested our silirenes in a photo-mediated reaction with triethylsilane in a model study by using <sup>1</sup>H and <sup>29</sup>Si NMR spectroscopy. For this, we mixed the reagents in *n*-hexane and irradiated the solution for 30 min at different wavelengths (254–420 nm). We observed the desired insertion reaction into the Si–H bond with the alkyl/aryl-substituted silirenes **E1–E3**; however, activation of these compounds was only achievable with hard UV-light (254 nm FLT). Thus, rendering this compound class ineffective for an application in silicone curing, since an activation above 280 nm is required. Although **E4** shows a distinct absorption maximum at 300 nm, no reaction at any given wavelength could be observed. Next, we investigated the group of silyl-substituted

silirenes **E7–E10**, due to their characteristic absorbance at higher wavelengths above 325 nm. This time activation and subsequent insertion of the silirene was performed with a 365 nm LED. In the case of **E7** even radiation at 420 nm could be employed with equal results. While silyl substituents shift the activation towards higher wavelength, the selectivity of the photoreaction decreases. The formation of an additional side product was observed, which could be assigned to the respective rearrangement product **Re** of the silirene. This type of rearrangement is known in literature for silyl- and hybrid-substituted silirenes in particular.<sup>[26]</sup> Unfortunately, the rearrangement product does not react further with any silane, hence reducing the capability of the silirene to crosslink Si–H functionalized polysiloxanes severely. To our surprise, silirenes **E7–E10** yielded in comparable product distributions. Relative ratios of approximately 33–66% were determined for the insertion/rearrangement products, which appears to be independent from the steric demand of the employed silyl-substituent. However, improved insertion ratios were measured by employing asymmetric silirenes **E13–E17**, substituted with both an alkyl/aryl- as well as a silyl-moiety. Due to the reduction to only one silyl-based, rearrangeable substituent in these scaffolds, the relative yield of the rearrangement reaction was significantly decreased to 34% under the described conditions. Nevertheless, activation of the respective silirenes was achieved at 365 nm, which meets our criteria for a UV-based curing process. Germyl-silirene **E18** afforded solely the respective rearrangement product under irradiation, while phosphine based silirenes **E19** and **E20** were entirely inactive towards any exposure of light in the range from 256 to 420 nm. It can be concluded that fully alkyl/aryl-substituted silirenes are unfit for our purpose, due to their low absorption and activation properties. Silyl-substituted silirenes show activation at higher wavelength but the primarily formation of the rearrangement product attenuate their effectiveness. By choosing asymmetric, aryl- and silyl-substituted silirenes the best compromise for both desired characteristics, possible activation above 300 nm and a higher selective photoreaction towards the insertion product, can be found. To further improve the photoreaction additional screenings were conducted to improve the reaction selectivity. (Table 2) For this optimization, silirene **E7** and **E14** were selected due to their described photo-activity, their good synthetic accessibility, and to represent the respective groups of disilyl- (**E7**) and aryl/silyl-substituted (**E14**) silirenes. First, a variation of the triethylsilane amount was investigated. In the absence of any silane the respective silirene reacts exclusively to the rearrangement product **Re**, without the formation of any other side products, whereas increasing the amount of silane from 2 to 10 or even 100 equiv. did not change in the reaction selectivity considerably. Hence, we assume that the reaction is not limited by reactant accessibility. Similar results can be concluded for the variation of the activation wavelength to 300 or 420 nm. Changing the solvent to toluene or cyclohexene also did not result in any notable shift. However, by reducing the reaction temperatures, we detected a significant change towards higher yields of the desired insertion product **In**. At –40 °C we observe that for **E7** both reaction products are

**Table 2.** Photoreaction of silirenes **E7** and **E14** with triethylsilane and variation of the reaction parameters to optimize the reaction selectivity.

| <br><b>E7</b> R = TMS<br><b>E14</b> R = Ph | In                   | Re7 R = TMS<br>Re14 R = Ph |                  |     |
|---|----------------------|----------------------------|------------------|-----|
|   |                      | In/Re <sup>[b]</sup> [%]   | E7               | E14 |
| Deviation from standard conditions  | t <sup>[a]</sup> [h] |                            |                  |     |
| none <sup>[c]</sup>   | 0.5                  | 34:66                      | 65:35            |     |
| 0 equiv. Et <sub>3</sub> SiH  | 0.5                  | 0:100                      | 0:100            |     |
| 10 equiv. Et <sub>3</sub> SiH   | 0.5                  | 34:66                      | 64:36            |     |
| 100 equiv. Et <sub>3</sub> SiH  | 0.5                  | 36:64                      | 65:35            |     |
| λ <sub>max</sub> = 300 nm   | 0.5                  | 35:65                      | 63:37            |     |
| λ <sub>max</sub> = 420 nm   | 0.5                  | 34:66                      | — <sup>[d]</sup> |     |
| toluene as solvent  | 0.5                  | 33:67                      | 65:35            |     |
| C <sub>6</sub> D <sub>12</sub> as solvent   | 0.5                  | 35:65                      | 64:36            |     |
| T = −40 °C  | 24                   | 50:50                      | 81:19            |     |
| T = −80 °C  | 72                   | 79:21                      | 93:07            |     |

[a] Reaction time was determined after full conversion of the respective silirene. [b] Relative yields were calculated via <sup>1</sup>H and <sup>29</sup>Si NMR spectroscopy by comparing the respective integrals. [c] Reaction conditions as written in scheme above. [d] No photo reaction at 420 nm could be observed.

present in equal shares, while the insertion product is formed predominantly with a relative ratio of 79% at a temperature of −80 °C. A similar tendency can be noted for **E14**, which afforded yields of the insertion greater than 90% at such low temperatures. Unfortunately, the improvement reaction selectivity is accompanied by a substantial increase in the reaction time. Full conversion of the respective silylene requires 24 h at −40 °C or even up to 72 h at −80 °C. Even though controlling the photoreaction through temperature bears great potential, the increase of the reaction time to several days and the actual implementation of a silicone curing process at −80 °C do not seem applicable or efficient. Hence, the most effective control to regulate the photoreaction stays the modification of the chemical scaffold itself.

### Si–OH photoreactivity

To evaluate the capability of our model system to react with silanols, silirene **E7** and **E14** were irradiated in the presence of triethylsilanol (Scheme 2). Again, we observed the photoreaction of both silirenes at 365 nm and the formation of the desired insertion, as well as the rearrangement product. The transient silylene inserts into the O–H bond of the silanol resulting in a siloxane, in contrast to the disilane formation in the reaction with triethylsilane. However, the respective rearrangement product, arising from the intramolecular reaction of the silirene, does not differ from the previous test reactions. Additionally, a second side reaction can be noted, which could be assigned to the ring-opening product. This literature known reaction is triggered by the increased nucleophilicity of the silanol compared to the silane.<sup>[15,27]</sup> Contrary to the rearrangement the ring-opening product does not reduce the curing efficiency of the silirene, since it creates a covalent bond with



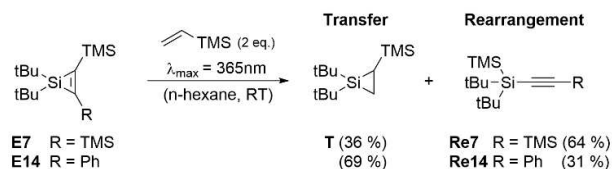
**Scheme 2.** Photoreaction of silirene **E7** and **E14** with triethylsilanol. Respective formation and relative ratio of the insertion, rearrangement, and ring-opening product.

the silanol. Consequently, curing with hydroxy-terminated silicones could be performed through both reactions, the insertion and the ring-opening. Again, silirene **E14** shows the higher selectivity towards the insertion product with 59% relative yield, while **E7** afforded only 29% relative yield.

Interestingly for both silirenes the respective ring-opening reaction occurred in comparable yields (13 and 14%, respectively). This could indicate a thermally induced reaction, which is not affected by the photoactivity of the silirene, since the ring-opening reaction is usually reported via heat control. To investigate this behavior, we conducted thermal control reactions. Heating the reaction mixtures up to 70 °C, no conversion of the silirenes could be detected over a period of 24 h. At temperatures above 80 °C small amounts of the ring-opening product were observable. By increasing the temperature to 110 °C the reaction could be accelerated to afford full conversion within 4 h. Even though **E7** and **E14** show a relatively high thermal stability towards triethylsilanol, we hypothesize that the irradiation and activation of the silirenes may facilitate this reaction even at lower temperatures. Additionally, reducing the reaction temperature to −40 °C results in an increase of the photoreaction selectivity. This time both relative yields of the rearrangement, and the ring-opening product were reduced to 16 and 5%, respectively, while the ratio of the insertion product was increased to 79% for the irradiation of **E14** under reduced temperature. Yet again, the respective reaction time increases likewise and durations of up to 30 h are required to afford full conversion under these conditions.

### Si–vinyl photoreactivity

At last, we studied the reactivity of silirene **E7** and **E14** towards vinyl-silanes to outline the curing potential for vinyl-functionalized polysiloxanes. Photoreactions were prepared by combining the respective silirene with vinyl-trimethylsilane. The mixtures were subsequently irradiated at 365 nm for 30 min and afforded the analogue rearrangement product as well as the desired transfer product (Scheme 3). This silylene-transfer-reaction

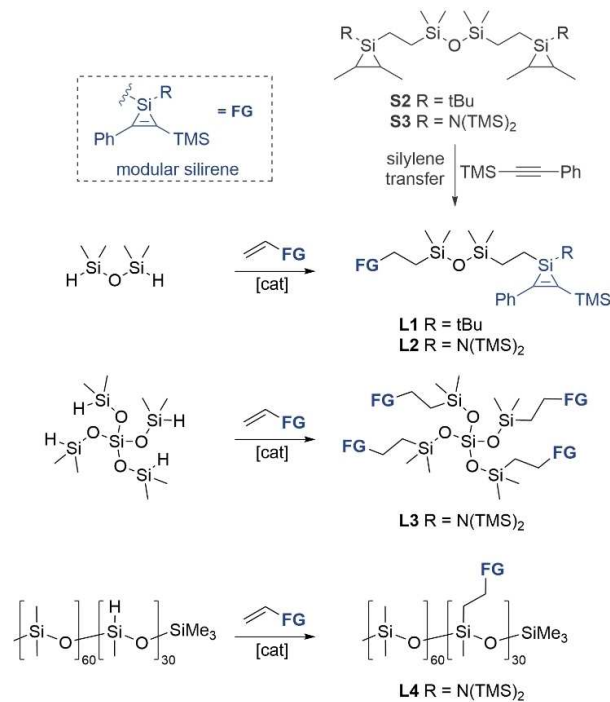


**Scheme 3.** Photoreaction of silirene **E7** and **E14** with vinyltrimethylsilane. Respective formation and relative ratio of the insertion and rearrangement product.

describes the transformation of a silirene to a silirane. As earlier described, these saturated silacycles lack the required photoactivity at higher wavelengths above 300 nm and will not react further under the employed irradiation at 365 nm once they are formed. Hence, the reaction with vinyl-triethylsilane results in the formation of the desired silirane product. Once again, we observed that **E14** affords higher yields in the photoreaction towards the transfer product with a relative yield of 69%, whereas **E7** results predominantly in the rearrangement product and only a relative ratio of 36% can be observed for the transfer reaction. In accordance with this, irradiating the reaction mixture at lower wavelengths ( $\lambda_{\text{max}}=265$  nm), resulted only in the formation of small amounts of the rearrangement product **Re** without the generation of any stable silirane. We presume that further decomposition of the intermediary formed silirane is caused by the use of hard UV-light, since this type of reactivity is well reported for siliranes at such low wavelengths.<sup>[28]</sup> Similar results could be obtained for the improvement of the photoreaction selectivity by reducing the reaction temperature. At  $-40^\circ\text{C}$  the relative yields of the transfer product were elevated to 78% for the light-mediated reaction of **E14**, while the reaction time was extended from 30 min to almost 30 h. We can summarize that our investigated silirenes **E7** and **E14** can react with the three mainly used silicone functionalities (Si–H, Si–OH, Si–vinyl) via photo-activation at 365 nm. The undesired side reaction (rearrangement) can be minimized by substitution of the silirene with both silyl- and aryl-moieties as well as by low temperature control.

### Crosslinker-scaffolds

In order to create effective curing agents, we need to generate multifunctional silirene structures. These can react with the provided functionalized polysiloxane chains and act as joints in the final silicone elastomer. Based on the obtained results from our model study, the motif of silirene **E14** was chosen as suitable candidate for these crosslinkers. As a result, the following multifunctional silirenes **L1–L4** have been synthesized accordingly (Scheme 4). We initially synthesized bifunctional silirenes **L1** and **L2** from the earlier reported<sup>[9]</sup> bifunctional silacyclopropanes **S2** and **S3** via the silylene transfer reaction as previously described for the model silirene compounds **E1–E20**. Best results were obtained through the thermally controlled reaction at  $120^\circ\text{C}$  and an excess of 3 equiv. of acetylene. However, this procedure was only applicable for bi- or trifunc-



**Scheme 4.** Synthesis of multifunctional silirene crosslinker **L1–L4** via silylene transfer or modular silirenes.

tional silirene scaffolds, due to the advancing complexity of the precursor synthesis with an increasing number of silirane-moieties. To tackle this issue, we recently reported a method to generate higher functional silirenes via the employment of “modular silirenes”.<sup>[29]</sup> Monofunctional silirene units can be grafted onto various Si–H-containing substrates, while avoiding the synthesis of complex precursors. Therefore, vinyl-functionalized silirenes were generated by substituting vinyl trichlorosilane with KHMDs (potassium hexamethyldisilazide) in a salt metathesis reaction to afford the vinyl dichloro-silane species. Subsequent reduction with a lithium/sodium alloy in the presence of 2-butene resulted in the formation of the vinyl-silirane, which was finally transformed into the “modular” vinyl-silirene via the silylene-transfer-reaction by employing the respective alkyne [1-phenyl-2-(trimethylsilyl)acetylene]. The “modular” silirene was then used in a hydrosilylation reaction with the presented hydrosilanes or PMHS. The employed hydrosilylation catalyst was subsequently removed by filtration through a combination of celite/ $\text{Al}_2\text{O}_3$ . A residue Pt concentration of less than 0.005 ppm could be detected by inductively coupled plasma optical emission spectroscopy (ICP-OES) measurements, demonstrating the successful separation of the noble metal from the product. This way, we were able to synthesize higher functional silirene crosslinker **L3** and polysiloxane-based linker **L4**. Additionally, bifunctional linker **L2** was re-synthesized via this procedure by combining tetramethyldisiloxane with the modular silirene to validate the applicability of this alternative method.

## Photo-curing

We tested the curing capability of our silirene based linkers L1–L4 in combination with different functionalized polysiloxanes. For this purpose, all commercially purchased polysiloxanes (Figure 1) were degassed and dried prior to the photocuring experiments. Heat and vacuum drying were sufficient for hydrid- and vinyl-terminated PDMS, while hydroxy-functionalized silicones were additionally filtered over dry neutral alumina and stored over 3 Å molecular sieve for several days. We employed polysiloxanes of comparable chain length with termination of Si–H (P1,  $n \approx 380$ ,  $M_w \approx 28 \text{ kg mol}^{-1}$ ), Si–OH (P2,  $n \approx 480$ ,  $M_w \approx 36 \text{ kg mol}^{-1}$ ), and Si–vinyl (P3,  $n \approx 380$ ,  $M_w \approx 28 \text{ kg mol}^{-1}$ ). Mixtures of PDMS and silirene-crosslinkers L1–L4 were combined under inert atmosphere and stirred until a homogenous phase was obtained. The respective mixtures were irradiated at 365 nm (LED) for several hours to afford the hardening of the employed silicones. Linker L1 and L2 were not able to form an elastomer with polysiloxane P1 in mixing ratios of  $R=0.5$ , 1, 2, or 4 ( $R$ =number of silirene-moieties/number of PDMS functional groups). This is no surprise, since bifunctional linkers can only yield in a chain elongation with terminated silicones. Presumably, this can be attributed to the described issue of forming a rearrangement product during the photo-reaction. Due to its reduced efficiency, photo-curing with only two active silirene centers appears to be insufficient. It is noteworthy that the crosslinker L2 was much better miscible with the employed silicones compared to L1. We suspect that the *tert*-butyl moiety experiences more repulsion in the PDMS matrix in contrast to the silazane  $[\text{N}(\text{TMS})_2]$  group of L2. Furthermore, no elastomer formation was observed by utilizing crosslinker L3 in combination with P1, however an increase of viscosity for the irradiated sample was detected. We surmise that the increase of silirene groups partly enables to combine the respective PDMS chains, leading to a chain elongation. Hence, resulting in an increase of viscosity, without forming a silicone network. We further investigated the curing process in an oscillatory rheometer, modified with a lower glass-plate to allow simultaneous irradiation with different LEDs and monitoring of the curing event. This way, we were able to observe not only an increase of the respective complex viscosity  $|\eta^*|$  of L3 with hydride terminated PDMS P1, but also an increase in the loss modulus  $G''$ , while no significant change in the storage modulus  $G'$  was detectable (Figure 2). This further supports the assumption of a chain elongation rather than a network formation. Nevertheless, utilizing the polymeric silirene linker L4 with hydride terminated silicone P1 resulted in successful curing of the linear polymer chains. For all mixing ratios ( $R=0.8$ ,

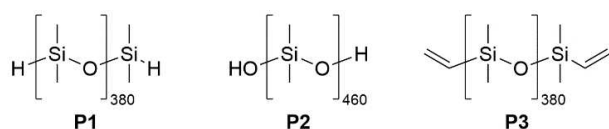


**Figure 1.** Terminal functionalized PDMS P1–P3 utilized for photocuring with silirene-based linkers.

1, and 2) of linker to PDMS the solidification could be observed. The curing speed of the afforded elastomers is dependent on the employed ratio. Thus, fastest hardening was observed with the highest tested ratio of  $R=2$ , which reached the sol–gel point  $[\tan(\delta)=1]^{[30]}$  at 47 min, while almost 6.5 h were required in the case of  $R=0.8$  to reach this transition point. This ratio  $R$  represents the minimal concentration of linker for which a successful curing could be observed, we did not obtain any elastomers below this ratio. Additionally, by varying the silirene ratio  $R$ , the final elastomer properties can be modified as well. The complex viscosity  $|\eta^*|$  increases from  $102 \text{ Pa s}^{-1}$  for  $R=0.8$  to  $1540 \text{ Pa s}^{-1}$  for  $R=2$ , indicating a denser network with increasing ratio. The dissipation factor  $\tan(\delta)$  decreases from 0.78 to 0.21, which implies an increase in the elasticity of the final elastomer (Figure 2, left graphic). Thus, we can conclude that with higher linker concentrations we obtain denser cured silicone elastomers.

Furthermore, curing of hydroxy-terminated PDMS P2 and vinyl-terminated PDMS P3 with L4 was feasible as well under equal conditions. Elastomers resulting from hydroxy-functionalized PDMS P2 shared similar properties to the ones originating from P1. In comparison, this curing proceeded generally slower, which can be shown by reaching the respective sol–gel transition point at extended times. For example, the crossing of  $\tan(\delta)=1$  for L4 with P2 with a ratio  $R=2$  occurred after 135 min, while a low ratio of  $R=0.8$  delayed this transition to 8.6 h. Yet, after the finalization of the photocuring, the final dissipation factors  $\tan(\delta)$  were obtained in a similar range from 0.93 to 0.32 (from  $R=0.8$  to 2), compared to elastomers created from P1. To our surprise, crosslinking of vinyl-terminated PDMS P3 with L4 proceeded much faster in all employed mixing ratios.

In contrast to before, P3 at a ratio of  $R=2$  solidified already after 28 min, almost half the required time for curing of P1 at the same conditions. Even at a substoichiometric ratio of  $R=0.8$  the transition point was reached within 125 min, indicating the accelerated curing process. Further, final dissipation factors ranging from 0.23 to 0.05, indicating a more elastic rubber product in comparison. We hypothesize that the  $[2+1]$  cyclo-addition to the respective silirane proceeds faster compared to the insertion reaction into either the Si–H or Si–OH bond in the polysiloxane, thus resulting in this observable difference in the curing speed. Nevertheless, the resulting elastomers afforded comparable final viscosities. For instance, the complex viscosity  $|\eta^*|$  of P3 at  $R=2$  resulted in a value of  $2656 \text{ Pa s}$  compared to  $2688 \text{ Pa s}$  for P2. Combining these results, we were able to cure these three different siloxane moieties with one crosslinker structure on the basis of multifunctional silirenes. This way, all tested linear polysiloxanes could be transformed into the respective elastomers via soft UV-irradiation under metal-free conditions. As additional proof for the light-mediated nature of the crosslinking process, we repeated the curing experiments of all three silicones P1–P3 with discontinuous irradiation periods. We could observe in all cases an increase of the storage modulus during irradiation, while deactivating the light source resulted in flattening of the respective modulus rate. By switching the light back on, the storage modulus continued to

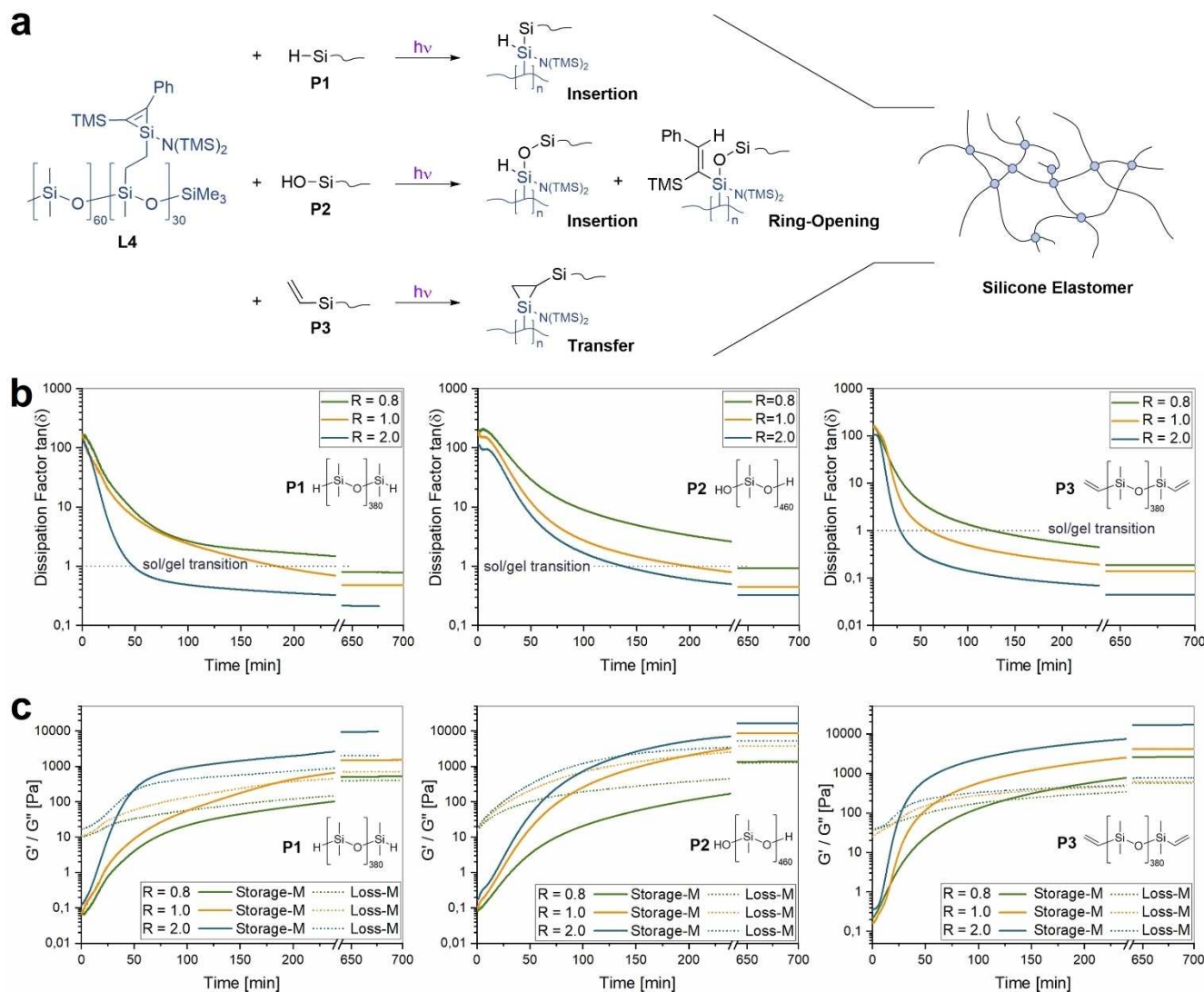


**Figure 2.** Photo-curing of terminal functionalized PDMS **P1**–**P3** with multifunctional silirene linker **L4**. (a) Proposed crosslinking reactions of linker **L4** with hydride- (**P1**), hydroxy- (**P2**), and vinyl- (**P3**) functionalized PDMS. (b) Dissipation factor  $\tan(\delta)$  vs. curing time with the depicted sol-gel transition point at  $\tan(\delta) = 1$  measured by oscillatory rheology ( $f = 1$  Hz,  $\gamma = 5\%$ ) for the photo-curing of linker **L4** with PDMS **P1**–**P3** at silirene/PDMS-moiety ratios  $R$  of 0.8–2.0. (c) Storage  $G'$  and loss modulus  $G''$  vs. curing time for the respective curing reactions of linker **L4** with PDMS **P1**–**P3** at silirene/PDMS-moiety ratios  $R$  of 0.8–2.0.

raise again, demonstrating the propagation of the respective curing.

## Conclusion

Herein we demonstrated the photo curing of linear polysiloxanes by employing multifunctional silirenes as crosslinkers, which serves as an alternative curing method. Initial investigation of small monofunctional silirenes in a model study provided evidence for the photolability and reactivity with the utilized functionalities. Substitution of the three-membered ring-system allowed effective tunability towards required absorption properties. Undesired rearrangement reactions via the photo-activation could be attenuated by minimizing silyl-

substitution or reduction of the reaction temperature. Based on these results, silirene **E14** was chosen as the most suitable chemical motif for the following curing agents. Multifunctional silirenes **L1**–**L4** were successfully obtained either via the silylene transfer reaction or utilization of modular silirenes. Bifunctional linkers **L1** and **L2** and tetrafunctional linker **L3** were unable to create any silicone elastomers due to the reduced reaction selectivity caused by the formation of the rearrangement product. Polymeric linker **L4** compensates this issue by introducing a higher number of silirenes per linker-scaffold, and finally enables a light-mediated curing of silicones. Reproducible curing of hydride-, hydroxy-, or vinyl-functionalized polysiloxanes allows a versatile application for the most common silicone moieties used in industry, without the use of any metal-based catalyst. Mechanical properties of the elasto-

mers can be controlled by the mixing ratios. Employing higher concentrations of crosslinker L4 resulted in faster cured, harder silicone rubbers. Further, it was shown that the curing duration is dependent on the utilized polydimethylsiloxane (PDMS) functionalities. Longest irradiation times were required for the curing of hydroxy-terminated PDMS, while fastest solidification occurred for vinyl-functionalized PDMS. The presented method provides exemplary structures for this type of curing, yet additional modifications are required to further improve its efficiency in terms of synthesis, stability, or reaction rates. Especially the suppression of the rearrangement side reaction would help to considerably enhance the curing capability. Nevertheless, the presented results provide the proof of concept for a light controlled, metal- and additive-free curing process through multifunctional silirenes. Additionally, a major advantage is the broad applicability of the silirene linkers towards different PDMS functionalities. In summary, these features result in a genuine alternative to the conventional catalyst or heat-based curing methods.

## Acknowledgements

We acknowledge our principal funding source for this work, the WACKER Chemie AG. Dr. Wolfgang Schindler, Dr. Maximilian Moxter and Dr. Niklas Wienkenhöver are acknowledged for helpful discussions and advice. Open Access funding enabled and organized by Projekt DEAL.

## Conflict of Interest

The authors declare the following conflicts of interest: One patent application was filed (PCT/EP2021/064438) covering the methods reported in this paper.

## Data Availability Statement

The data that support the findings of this study are available in the supplementary material of this article.

**Keywords:** metal-free · photo-curing · polysiloxanes · silacyclopropene · silylene

- [1] a) *Silicon in organic, organometallic, and polymer chemistry* (Ed.: M. A. Brook), Wiley, New York, **2000**; b) *Thermal Properties of Polysiloxanes* (Ed.: P. R. Dvornic), Springer, Dordrecht, **2000**; c) J. E. Mark, D. W. Schaefer, G. Lin, *The polysiloxanes*, Oxford University Press, New York, **2015**.
- [2] a) *Handbook of thermoset plastics* (Ed.: H. Dodiuk), William Andrew, Norwich, **2022**; b) M. Androit, *Silicones in industrial applications*, Inorganic Polymers, **2007**.
- [3] GrandViewResearch Inc., *Silicone Market Size, Share & Trends Analysis Report by Product, by End-use, by Region, And Segment Forecasts, 2021–2028*, Report ID: GVR-1-68038-063-7, **2020**.

- [4] *Polymer handbook* (Eds.: J. Brandrup, E. H. Immergut, E. A. Grulke, A. Abe, D. Bloch), Wiley, New York, **1999**.
- [5] I. E. Markó, S. Stérin, O. Buisine, G. Berthon, G. Michaud, B. Tinant, J.-P. Declercq, *Adv. Synth. Catal.* **2004**, *346*, 1429.
- [6] National Research Council, *The Role of the Chemical Sciences in Finding Alternatives to Critical Resources: A Workshop Summary*, The National Academies Press, Washington D. C., **2012**.
- [7] M. Y. Wong, A. F. Schneider, G. Lu, Y. Chen, M. A. Brook, *Green Chem.* **2019**, *21*, 6483.
- [8] G. Lu, A. F. Schneider, M. Vanderpol, E. K. Lu, M. Y. Wong, M. A. Brook, *Ind. Eng. Chem. Res.* **2021**, *60*, 15019.
- [9] F. A. D. Herz, M. Nobis, D. Wendel, P. Pahl, P. J. Altmann, J. Tillmann, R. Weidner, S. Inoue, B. Rieger, *Green Chem.* **2020**, *22*, 4489.
- [10] K. Goswami, A. L. Skov, A. E. Daugaard, *Chem. Eur. J.* **2014**, *20*, 9230.
- [11] R. Sønderbæk-Jørgensen, S. Meier, K. Dam-Johansen, A. L. Skov, A. E. Daugaard, *Macromol. Mater. Eng.* **2022**, 2200157.
- [12] C. Choi, J. L. Self, Y. Okayama, A. E. Levi, M. Gerst, J. C. Speros, C. J. Hawker, J. Read de Alaniz, C. M. Bates, *J. Am. Chem. Soc.* **2021**, *143*, 9866.
- [13] R. T. Conlin, P. P. Gaspar, *J. Am. Chem. Soc.* **1976**, *98*, 3715.
- [14] a) F. Lips, A. Mansikkamäki, J. C. Fettinger, H. M. Tuononen, P. P. Power, *Organometallics* **2014**, *33*, 6253; b) S. Ishida, T. Iwamoto, M. Kira, *Heteroat. Chem.* **2011**, *22*, 432; c) J. A. Baus, N. Laskowski, R. Tacke, *Chem. Ber.* **2016**, *2016*, 5182; d) Y. E. Türkmen in *Comprehensive Heterocyclic Chemistry IV* (Ed.: D. Black), Elsevier Science & Technology, San Diego, **2022**, pp. 506–533.
- [15] M. Ishikawa, A. Naka, J. Ohshita, *Asian J. Org. Chem.* **2015**, *4*, 1192.
- [16] a) J. Ohshita, N. Honda, K. Nada, T. Iida, T. Mihara, Y. Matsuo, A. Kunai, A. Naka, M. Ishikawa, *Organometallics* **2003**, *22*, 2436; b) M. Ishikawa, K. Nishimura, H. Sugisawa, M. Kumada, *J. Organomet. Chem.* **1980**, *194*, 147; c) M. Ishikawa, H. Sugisawa, M. Kumada, H. Kawakami, T. Yamabe, *Organometallics* **1983**, *2*, 974.
- [17] a) M. Ishikawa, H. Sugisawa, T. Fuchikami, M. Kumada, T. Yamabe, H. Kawakami, K. Fukui, Y. Ueki, H. Shizuka, *J. Am. Chem. Soc.* **1982**, *104*, 2872; b) A. Sekiguchi, T. Tanaka, M. Ichinohe, K. Akiyama, S. Tero-Kubota, *J. Am. Chem. Soc.* **2003**, *125*, 4962; c) D. Seyferth, S. C. Vick, *J. Organomet. Chem.* **1977**, *125*, C11.
- [18] a) L. Wang, Y. Li, Z. Li, M. Kira, *Coord. Chem. Rev.* **2022**, *457*, 214413; b) C. Shan, S. Yao, M. Drieß, *Where silylene-silicon centres matter in the activation of small molecules*, Technische Universität Berlin, **2020**.
- [19] R. R. Aysin, L. A. Leites, S. S. Bukalov, *Organometallics* **2020**, *39*, 2749.
- [20] M. S. Gordon, *J. Am. Chem. Soc.* **1980**, *102*, 7419.
- [21] a) T. Roychowdhury, C. V. Cushman, R. A. Synowicki, M. R. Linford, *Surf. Sci. Spectra* **2018**, *25*, 26001; b) D. Cai, A. Neyer, R. Kuckuk, H. M. Heise, *J. Mol. Struct.* **2010**, *976*, 274.
- [22] P. Boudjouk, E. Black, R. Kumarathasan, *Organometallics* **1991**, *10*, 2095.
- [23] S. Qiu, C. Zhang, R. Qiu, G. Yin, J. Huang, *Adv. Synth. Catal.* **2018**, *360*, 313.
- [24] R. West, L. C. Quass, *J. Organomet. Chem.* **1969**, *18*, 55.
- [25] a) S. Sekigawa, T. Shimizu, W. Ando, *Tetrahedron* **1993**, *49*, 6359; b) W. Uhlig, *J. Organomet. Chem.* **1997**, *545–546*, 281.
- [26] a) T. J. Barton, G. T. Burns, *Tetrahedron Lett.* **1983**, *24*, 159; b) M. Zielinski, M. Trommer, W. Sander, *Organometallics* **1999**, *18*, 2791; c) T. J. Barton, S. A. Burns, G. T. Burns, *Organometallics* **1983**, *2*, 199; d) M. Trommer, W. Sander, C. Marquard, *Angew. Chem. Int. Ed.* **1994**, *33*, 766.
- [27] M. Ishikawa, T. Fuchikami, M. Kumada, *J. Am. Chem. Soc.* **1977**, *99*, 245.
- [28] a) P. Boudjouk, U. Samaraweera, R. Sooriyakumaran, J. Chrusciel, K. R. Anderson, *Angew. Chem. Int. Ed.* **1988**, *27*, 1355; b) M. Ishikawa, M. Kumada in *Advances in Organometallic Chemistry* (Eds.: F. Stone, R. West), Academic Press, **1981**, pp. 51–95.
- [29] M. Nobis, S. Inoue, B. Rieger, *Chem. Commun.* **2022**, *58*, 11159.
- [30] T. G. Mezger, *The Rheology Handbook*, Vincentz Network, **2012**.

Manuscript received: October 21, 2022

Revised manuscript received: November 20, 2022

Accepted manuscript online: November 29, 2022

Version of record online: December 19, 2022